

SOUNDS IN SPACE: THE POTENTIAL USES FOR ACOUSTICS IN THE EXPLORATION OF OTHER WORLDS

TIMOTHY LEIGHTON¹, ANDI PETCULESCU²

¹ Institute of Sound and Vibration Research, University of Southampton,
Highfield, Southampton SO17 1BJ, UK
tgl@soton.ac.uk

² Department of Physics, University of Louisiana – Lafayette,
PO Box 44210, Lafayette, LA 70504, USA
andi@louisiana.edu

This paper examines the past and future uses for acoustics in space research. Whilst on the larger scales in some topic areas, acoustical models have proved to be useful in extraterrestrial research, in other areas there has been not so much use made of acoustical techniques. One particular area where greater use might be made of acoustical sensors is in the deployment of acoustical sensors on probes sent out to other moons and planets. This is surprising given that acoustical sensors deliver benefits that are particularly useful for planetary probes, in terms of weight, bandwidth, ruggedness and cost. Whilst geoacoustical data could be obtained from many bodies, those which contain a dense atmosphere or an ocean offer intriguing additional possibilities. Examples from Mars, Venus, Titan, Enceladus and Europa will be discussed.

INTRODUCTION

January 2005 marked what was, for most astroacousticians, the opportunity to hear, for the first time, microphone signals from another world that were generated through pressure fluctuations at source. The outstanding achievement of the Huygens team in obtaining such data has, perhaps, opened up a new era for the use of acoustic sensors in the exploration of other worlds [1]. In addition to the passive microphone records, the Huygens probe generated its own acoustic signals in order to measure the atmospheric sound speed, and the distance to Titan's surface, primarily through time-of-flight measurements [2 - 7].

Throughout the history of space exploration, an impressive suite of sensors has been launched on probes for extraterrestrial research. However whilst camera systems are almost ubiquitous, most probes have lacked any sensitivity to sound. Whilst acoustic information cannot compete with images for human interpretation, sound in the absence of vision contains complementary information that we often take for granted in many aspects of human life (from diagnosing the performance of a car engine as we drive, to estimating the ferocity of a rainstorm on the bedroom window at night, to monitoring the happiness of a baby hidden beneath the canopy of a pram). By demonstrating that, by using our limited knowledge of the environmental conditions on another world, we can predict the way sounds are generated and propagate on those worlds, we can demonstrate the potential for undertaking a far more useful calculation: that is, specifically, the ability to diagnose the properties of the environments on other worlds from the sounds which a probe might detect. Such demonstrations are vital to give impetus for equipping future probes with microphones.

To date, four missions have carried microphones: the Venera expeditions to Venus [8-10], the Cassini-Huygens mission to Titan [2, 3], and the Mars Polar Lander (although contact was lost with the probe before deployment) [11, 12]. By developing increased abilities to predict the acoustic properties of other worlds, we can demonstrate the growing potential for inverting active and passive acoustic measurements to explore those worlds in a valuable manner which is complementary to the imaging systems that have proved to be so useful in past decades.

The Venera 13 and 14 landers pioneered the use of microphones, which were initially intended to listen for lightning. The acquired data was inconclusive, most of the recorded sounds having been generated by air flow past the lander. Subsequent efforts to infer the wind speed from the acoustic data yielded speeds between 0.35 and 0.57 m/s [10]. More recently, the Huygens lander employed both passive and active acoustic sensors. The passive sensors – microphones – recorded sounds from the probe's descent through Titan's atmosphere [6]. Two sets of active sensors were incorporated in Huygens: a transmitter-receiver (T/R) sound speed sensor and an acoustic array. The T/R sensor measured the ambient sound speed via the time of flight. The array measured the acoustic time of flight between the probe and the ground. These measurements were used to determine the probe's velocity and also for surface profiling [7].

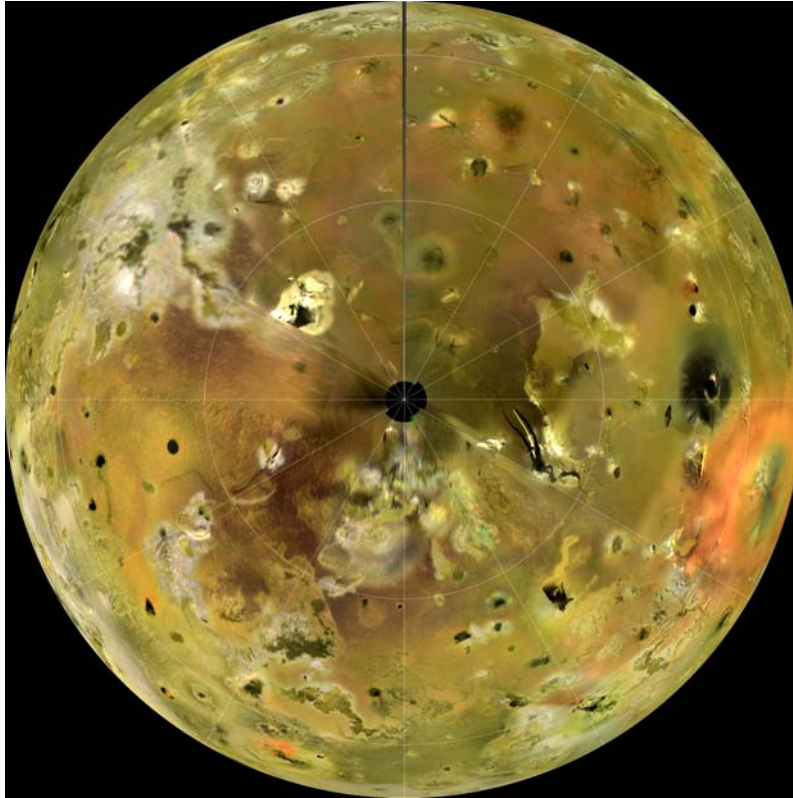
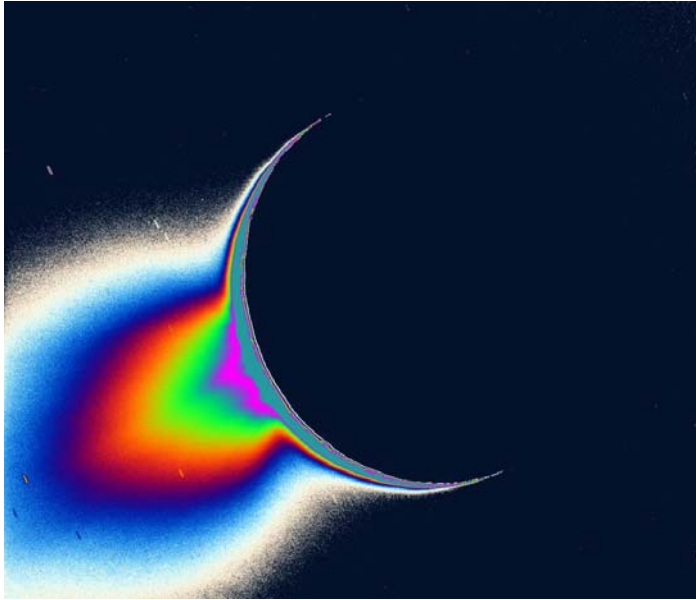


Fig.1 Io is the most volcanically active body in the Solar System. Volcanoes erupt massive volumes of silicate lava, sulphur and sulphur dioxide, constantly changing Io's appearance. Images have been produced by combining the best images from both the Voyager 1 and Galileo Missions. This image shows the South Polar regions of Io. The massive red deposit around Pele is the most distinctive expression of volcanic activity on Io. This image is provided courtesy of NASA/JPL (original in colour), and the caption is based on text supplied by NASA



(a)



(b)

Fig.2 (a) Cassini images of Saturn's moon Enceladus backlit by the sun show the fountain-like sources of the fine spray of material that towers over the south polar region. The image was taken using the Imaging Science Subsystem (Narrow Angle), looking more or less broadside at "tiger stripe" fractures Enceladus images. It shows discrete plumes of a variety of apparent sizes above the limb of the moon. The greatly enhanced and colored image shows the enormous extent of the fainter, larger-scale component of the plume. Imaging scientists, as reported in the journal *Science* on March 10, 2006, believe that the jets are geysers erupting from pressurized subsurface reservoirs of liquid water above 273 degrees Kelvin (0 degrees Celsius). (b) Cassini imaging scientists used views like this one to help them identify the source locations for individual jets spurting ice particles, water vapour and trace organic compounds from the surface of Saturn's moon Enceladus. Their study -- published in the Oct. 11, 2007, issue of the journal *Nature* -- identifies eight source locations, all on the prominent tiger stripe fractures, or sulci, in the moon's south polar region. Some of the sources occur in regions not yet observed by Cassini's composite infrared spectrometer, and the researchers predict that future Cassini observations of those locations will find elevated temperatures. This false-colour view was created by combining three clear filter images taken at nearly the same time as the image shown in (a). This image product was then specially processed to enhance the individual jets that compose the plume (the image shown in (a) was instead processed to reveal subtleties in the brightness of the overall plume that comprises the jets). Some artefacts due to the processing are present in the image. The final product was coloured as blue for dramatic effect. The images were acquired with the Cassini spacecraft narrow-angle camera on Nov. 27, 2005 at a distance of approximately 148,000 kilometers (92,000 miles) from Enceladus and at a sun-Enceladus-spacecraft, or phase, angle of 161 degrees. Scale in the original images is about 880 meters (0.5 mile) per pixel. This view has been magnified by a factor of two from the original images. These images were provided courtesy of NASA/JPL (original in colour) and the caption is based on text from NASA

1. WHAT CONSTITUTES AN EXTRATERRESTRIAL ACOUSTICAL SIGNAL

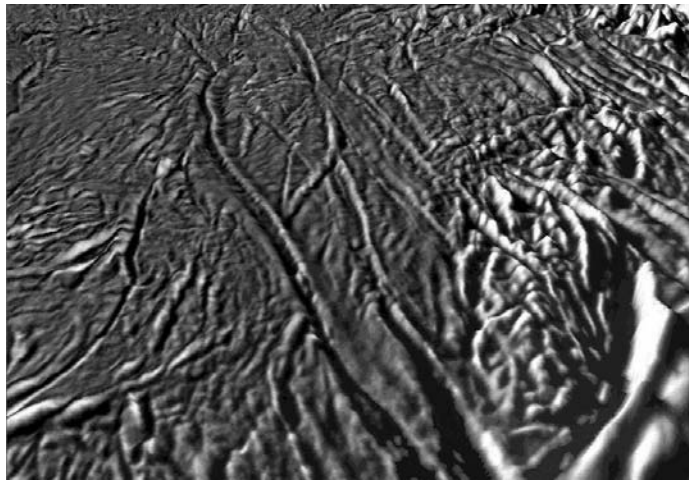
There are four main ways in which acoustics has entered extraterrestrial exploration [13]. These are listed below in a subjective assessment of the interest they might hold to a physical acoustician.

Artificial acoustic time-series have been constructed from signals associated with extraterrestrial phenomena. That is to say, sound can be used as the medium through which some other time-varying non-acoustic signal (such as radio waves generated by Jovian lightning) is communicated to humans. Examples can be found at web site reference [14]. EM signals detected on non-acoustic sensors can be played as audio sound files, regardless of whether their source is acoustic or not. Whilst in many cases the physical phenomenon at the source of this emission may have little or no relevance to acoustics, there are examples where there have been some acoustical perturbations involved in the generation of the signal. This connection perhaps adds extra relevance when the signals are conveyed acoustically to humans. An example of this can be found in the construction of an audio signal from the fluctuations in the cosmic background radiation which are thought to be related to acoustical fluctuations in the early expanding universe 14 billion years ago [15 -18]. Whilst a great many of the phenomena can be thought of as having a source with an ‘acoustical footprint’ (lightning, bow shock waves in the solar wind caused by the passage of a planet etc.), it is important to distinguish to what extent that ‘acoustical footprint’ is translated into the detected signal (e.g. electrical pickup from lightning does not directly tell us about the acoustical signal we would have heard from the thunder).

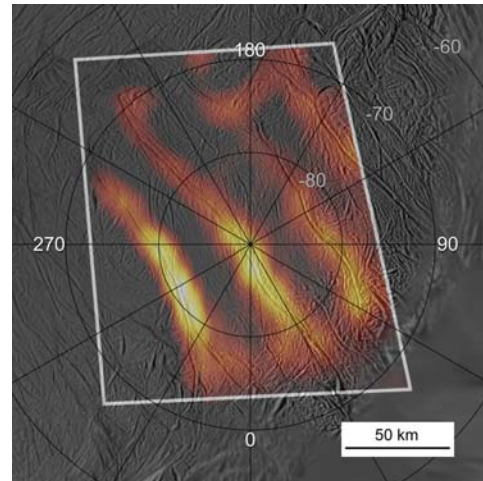
A more direct link to acoustics is found when perturbations in a non-acoustic signal (e.g. EM) are interpreted through mechanisms relating to acoustic perturbations in the source material itself. These traditional extraterrestrial acoustical investigations have been dominated by the use of models of infrasonic waves in order to interpret perturbations in EM data. Examples include modal acoustic waves in planets [19] and stars [20, 21], which may for example identify the existence of planets or, in our own solar atmosphere, to investigate solar dynamics [22, 23]; and in dust plasmas such as occur in planetary rings, comets, noctilucent clouds [24 -29].

A more direct link to acoustics would be found in those probes that make direct measurements of acoustic signals which have been generated by the probe itself, such as by inferring the local atmospheric sound speed from the time-of-flight of an acoustic pulse over a short distance ($O(10\text{ cm})$). To the authors’ knowledge, the Huygens probe is the only one of this kind to date. The Huygens sound speed measurements were used to assess the concentration of methane in Titan’s atmosphere [6]. The Huygens lander also incorporated a SODAR (SOund Detection And Ranging) array [7] that was used to measure the distance to ground and assess the condition of the landing zone during the probe’s descent [3].

In principle, with an appropriate propagation model, the received acoustic signal can be interpreted (inverted) to estimate the properties of the source and the propagation path. For probes which transmit and receive artificially-generated acoustic pulses, the source is well-known and the interpretation reveals details of the propagation medium. This might range from inferring atmospheric sound speed from time-of-flight measurements over a few cm [2] to, speculatively, propagation around entire planets [30,31], a topic which at the lower frequency limit merges with that of modal oscillations of the planet or star itself [32-34] (as described above). There is a special class of sensor which would monitor the natural sounds generated by the alien world itself. These are discussed in Section 3.



(a)



(b)

Fig. 3 (a) The plumes of water and other ice vapours (shown in Figure 2 jetting from the surface of Enceladus) originate from long linear fractures near the south pole of Enceladus, a geologically young and active region. This perspective view shows several of these “tiger stripes” from which the plumes are venting. The stripes themselves consist of deep grooves flanked by two elevated ridges. The south polar terrains generally are also heavily fractured and deformed. These new topographic maps, constructed from stereo and shape-from-shading techniques by Dr. Paul Schenk (<http://www.lpi.usra.edu/lpi/schenk/>) at the Lunar and Planetary Institute, show that the stripes do not have a great deal of relief. The flanking ridges are typically 75 to 200 meters high while the grooves in between the ridges are 150 to 300 meters deep.

Intensely deformed ridges along the edge of the south polar terrains (lower right) have relief of up to 1 kilometer or so. Vertical relief has been exaggerated by a factor of 20 in this view to aid interpretation. (b) Heat radiating from the entire length of 150 kilometer (95 mile)-long fractures is seen in this heat map of the active south polar region of Saturn's ice moon Enceladus. The warmest parts of the fractures tend to lie on locations of the plume jets. The measurements were obtained by the Cassini spacecraft's Composite Infrared Spectrometer from the spacecraft's close flyby of the moon on March 12, 2008. Remarkably high temperatures, at least 180 Kelvin (minus 135 degrees Fahrenheit) were registered along the brightest fracture, named Damascus Sulcus, in the lower left portion of the image. For comparison, surface temperatures elsewhere in the south polar region of Enceladus are below 72 Kelvin (minus 330 degrees Fahrenheit). Heat is escaping from Enceladus' interior along these warm fractures, dubbed "tiger stripes," which are also the source of the geysers that erupt from the polar region. The infrared radiation was mapped at wavelengths between 12 and 16 microns. The infrared data, shown in false color, are superimposed on a grayscale image mosaic of the south pole obtained by Cassini's cameras on July 14, 2005, during the previous close Enceladus flyby. Numbers on the map indicate latitude and longitude.

This new view shows that at least three of the south polar fractures are active along almost their full lengths—the fourth one, on the right, was only partially covered by this scan. The level of activity varies greatly along the fractures. The warmest parts of the fractures tend to lie on locations of the plume jets identified in earlier images. The main "tiger stripe" fractures are not the only sources of heat, however; additional warm spots are seen in the upper right part of the scan. The warm regions are probably concentrated within less than a few hundred meters (a few hundred yards) of the fractures, and their apparent width in this image results from the relatively low resolution of the infrared data. This map was made by scanning the south pole during the period from 16 to 37 minutes after closest approach to

Enceladus, at a distance between 14,000 and 32,000 kilometers (about 8,700 and 20,000 miles) as Cassini rapidly receded from its close (50-kilometer or 32-mile) flyby. These images were provided courtesy of NASA/JPL (original in colour) and the caption is based on text from NASA

To conclude therefore, the question of what constitutes an extraterrestrial acoustic signal is not a simple one. In many cases, the extraterrestrial signal may never have been in acoustical form until the time history is reconstituted as such via a loudspeaker for human listeners. Even where the signal is detected by an acoustic sensor, care is needed in its interpretation: both electromagnetic and mechanical pickup can appear to be acoustical in origin [35]. Even genuine pressure perturbations at a microphone should be categorised to distinguish which components are acoustical in origin (such that they would propagate to distance, for example between two microphones) and which are aerodynamic/hydrodynamic pressure fluctuations.

2. NATURAL SOUND SOURCES ON OTHER WORLDS

If the source of sound is natural, the power requirements and complexity of the hardware in principle become simpler. However the inversion discussed in Section 1 now contains an extra cause of uncertainty (i.e. the characteristics of the source), making it a much more demanding task for anything more than a rudimentary characterisation of the sound source (e.g. distinguishing between lightning and self-noise in the probe). Two key aspects to any future acoustical explorations of alien worlds by *in situ* probes are:

- appropriate design of the sensor (e.g. so that the aerodynamic/hydrodynamic and acoustical components of the signal can be separated; and to optimise the signal retrieval with limited bandwidth and dynamic range); and
- development of appropriate models of sound generation and propagation in the alien world (e.g. to predict the signal characteristics to inform sensor design (e.g. gain, dynamic range, the characteristics of the acoustical and inherent electrical noise); and to provide a basis for planning how to exploit those data, once collected, to interpret the environmental characteristics through inversion).

Models are under development for atmospheric propagation in gas giants [19, 32-34] and smaller planetary bodies [36 -41], and propagation in extraterrestrial ice [42, 43] and oceans [31]. Models are being developed for sound generation by liquid flows (e.g. ‘waterfalls’, splashes and waves) [44] and ice faults [45- 48].

3. CONCLUSIONS

From the volcanoes of Io (Figure 1) to the ‘dust devils’ of Mars [49,50], from the waters of Enceladus (Figures 2 and 3) and Europa (Figure 4) [31] to the lakes of Titan [51-53] (Figures 5-8), from the impacts of comets and asteroids [32-34, 54] to density fluctuations propagating in the solar wind, the Solar System is a dynamic environment which can reveal much through acoustics.

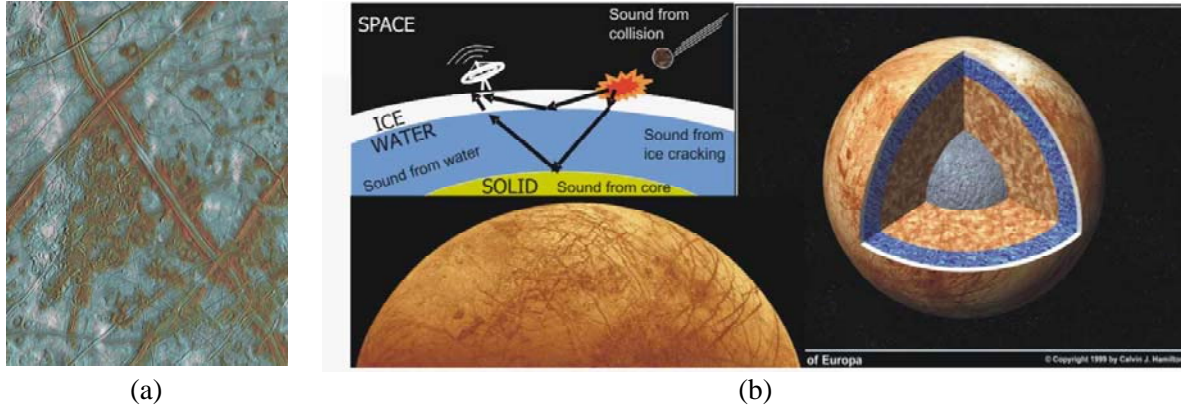


Fig.4 (a) Cracks on Europa's ice surface. Most scientists believe that salts and other inorganic materials are responsible for the coloured patches on Europa's outer layer, although there has been speculation that bacteria, extruded through the ice from below and 'flash frozen' on the surface, are responsible. (Credit: NASA/JPL) (b) Top left: schematic of possible acoustic-based mission to Europa, where acoustic signals originating from various planetary sources are passively detected and transmitted to Earth via an orbiter: ray paths and scales are for illustrative purposes only (schematic from reference [55]). Lower: the surface of Europa, showing ice features (Credit: NASA/JPL). Right: Schematic of the interior of Europa showing ice covering over a water ocean, overlaying the solid interior (Copyright Calvin J Hamilton). (Original in colour)

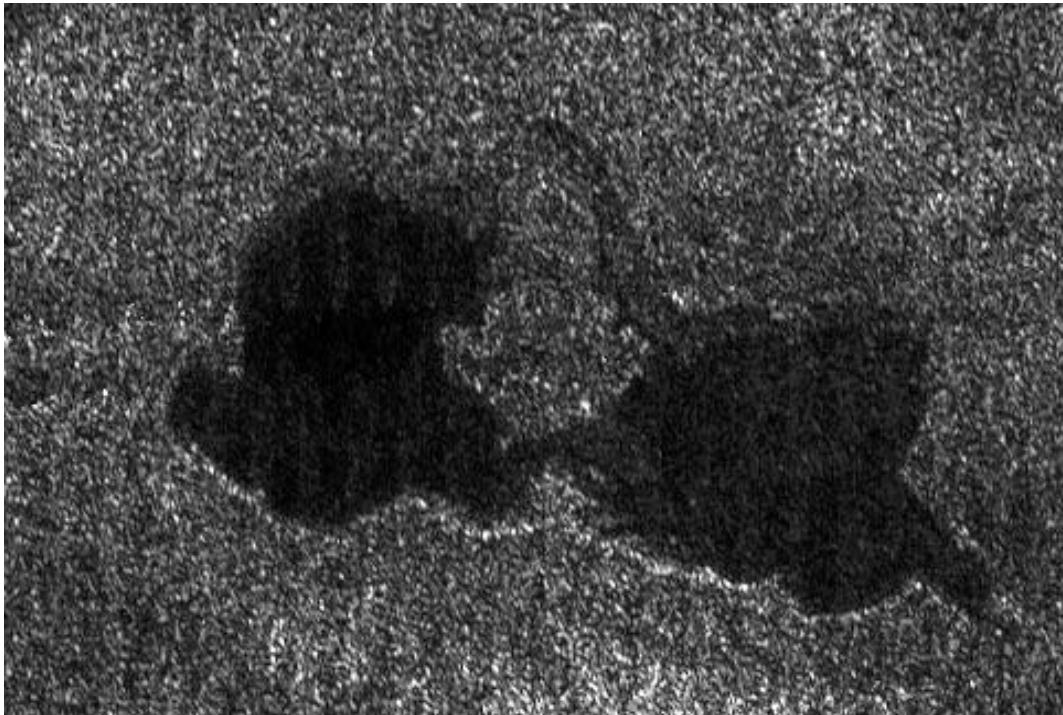
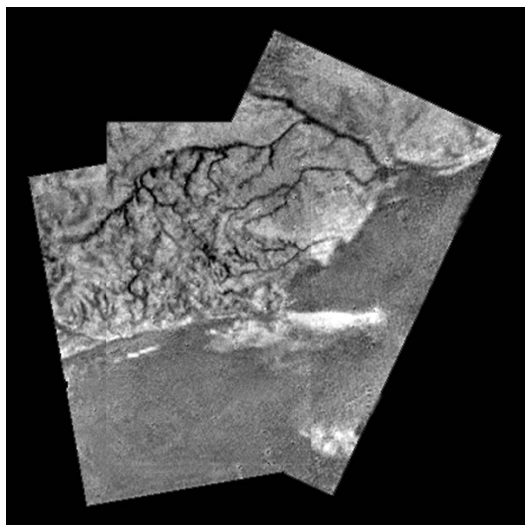


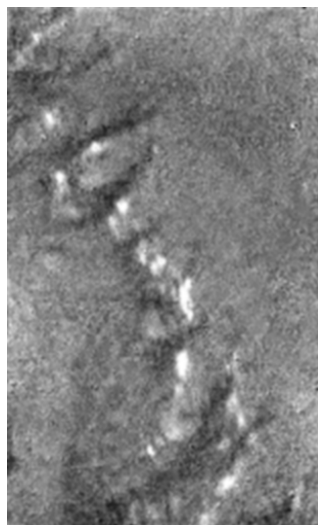
Fig.5 In this Cassini radar image, two of Titan's lakes (near 73 degrees north latitude, 46 degrees west longitude) are seen, each 20 to 25 kilometers (12 to 16 miles) across. The image from a flyby on Sept. 23, 2006, covers an area about 60 kilometers (37 miles) wide by 40 kilometers (25 miles) high. They are joined by a relatively narrow channel. The lake on the right has lighter patches within it, indicating that it may be slowly drying out as the northern summer approaches. This image is provided courtesy of NASA/JPL and the caption is based on text from NASA



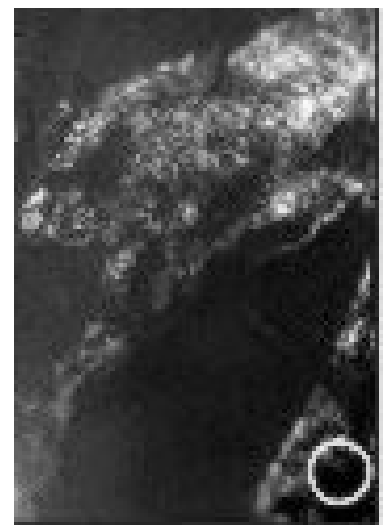
Fig.6 This side-by-side image shows a Cassini radar image (on the left) of what is the largest body of liquid ever found on Titan's north pole, compared to Lake Superior (on the right). This close-up is part of a larger image and offers strong evidence for seas on Titan. These seas are most likely liquid methane and ethane. This feature on Titan is at least 100,000 square kilometers (39,000 square miles), which is greater in extent than Lake Superior (82,000 square kilometers or 32,000 square miles), which is one of Earth's largest lakes. The feature covers a greater fraction of Titan than the largest terrestrial inland sea, the Black Sea. The Black Sea covers 0.085 percent of the surface of the Earth; this newly observed body on Titan covers at least 0.12 percent of the surface of Titan. Because of its size, scientists are calling it a sea. The image on the right is from the SeaWiFS project, NASA's Goddard Space Flight Center, Greenbelt, Md. (Image Credit: NASA/JPL/GSFC) (original in colour). The caption is based on text from NASA..



(a)



(b)



(c)

Fig.7 Images of Titan obtained by the Huygens probe. (a) This mosaic of three frames provides detail of a high ridge area including the flow down into a major river channel from different sources. (b) A single image from the Huygens DISR instrument of a dark plain area on Titan, seen during descent to the landing site. There appears to be flow around bright 'islands'. The areas below and above the bright islands may be at different elevations. (c) The landing site of Huygens is circled. (Credits: ESA/NASA/JPL/University of Arizona). The caption is based on text from NASA

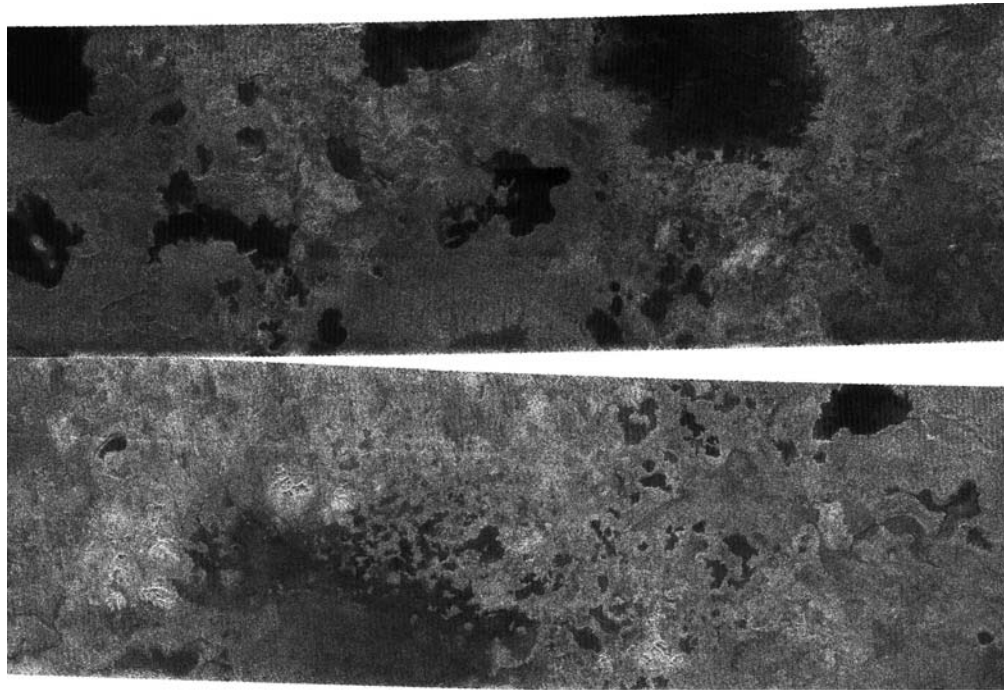


Fig.8 These two radar images were acquired by the Cassini radar instrument in synthetic aperture mode on July 21, 2006. The top image centred near 80 degrees north, 92 degrees west measures about 420 km by 150 km (260 miles by 93 miles). The lower image centred near 78 degrees north, 18 degrees west measures about 475 km by 150 km (295 miles by 93 miles). Smallest details in this image are about 500 meters (1,640 feet) across. The variety of dark patches in the image suggests the presence of many lakes in the high latitudes around the North Pole of Titan. Some of these dark patches have channels leading in or out of them. The channels have a shape that strongly implies they were carved by liquid. Some of the dark patches and connecting channels are completely black, that is, they reflect back essentially no radar signal, and hence must be extremely smooth. In some cases rims can be seen around the dark patches, suggesting deposits that might form as liquid evaporates. Because such lakes may wax and wane over time, and winds may alter the roughness of their surfaces, repeat coverage of these areas should test whether these are indeed bodies of liquid. (Image Credit: NASA/JPL). The caption is based on text from NASA

REFERENCES

1. H. Muir, Sounds in space. *New Scientist*, Vol. 195 (2616), 28-32, 2007.
2. J.P. Lebreton, O. Witasse, C. Sollazzo, T. Blancquaert, P. Couzin, A.-M. Schipper, J. B. Jones, D. L. Matson, L. I. Gurvits, D. H. Atkinson, B. Kazeminejad, M. Pérez-Ayúcar, An overview of the descent and landing of the Huygens probe on Titan, *Nature* Vol. 438, 758–764, 2005.
3. J. C. Zarnecki, M. R. Leese, B. Hathi, A. J. Ball, A. Hagermann, M. C. Towner, R. D. Lorenz, J. A. M. McDonnell, S. F. Green, M. R. Patel, T. J. Ringrose, P. D. Rosenberg, K. R. Atkinson, M. D. Paton, M. Banaszkiwicz, B. C. Clark, F. Ferri, M. Fulchignoni, N. A. L. Ghafoor, G. Kargl, H. Svedhem, J. Delderfield, M. Grande, D. J. Parker, P. G. Challenor, J. E. Geake, A soft solid surface on Titan as revealed by the Huygens Surface Science Package, *Nature* Vol. 438, 792-795, 2005.
4. M. Fulchignoni, F. Ferri, G. Colombatti, J. C. Zarnecki, H. M. Harri, M. Hamelin, J. J. Lopez-Moreno, K. Schwingenschuh, F. Angrilli, HASI Team, HASI Experiment to Titan, *Bulletin of the American Astronomical Society*, Vol. 37, 621, 2005 (abstract only).
5. M. Fulchignoni, F. Ferri, F. Angrilli, A. J. Ball, A. Bar-Nun, M. A. Barucci, C. Bettanini, G. Bianchini, W. Borucki, G. Colombatti, M. Coradini, A. Coustenis, S. Debei, P. Falkner, G. Fanti, E. Flamini, V. Gaborit, R. Gard, M. Hamelin, A. M. Harri, B. Hathi, I. Jernej, M. R. Leese, A. Lehto, P. F. Lion Stoppato, J. J. López-Moreno, T. Mäkinen, J. A. M. McDonnell, C. P. McKay, G. Molina-Cuberos, F. M. Neubauer, V. Pirronello, R. Rodrigo, B. Saggin, K. Schwingenschuh, A. Seiff, F. Simões, H. Svedhem, T. Tokano, M. C. Towner, R. Trautner, P. Withers, J. C. Zarnecki, In situ measurements of the physical characteristics of Titan's environment, *Nature* Vol. 438, 785-791, 2005.
6. A. Hagermann, P.D. Rosenberg, M.C. Towner, J.R.C. Garry, H. Svedhem, M.R. Leese, B. Hathi, R.D. Lorenz, J.C. Zarnecki, Speed of sound measurements and the methane abundance in Titan's atmosphere, *Icarus* Vol. 189, 538-543, 2007.
7. M.C. Towner, J.R.C. Garry, R.D. Lorenz, A. Hagermann, B. Hathi, H. Svedhem, B.C. Clark, M.R. Leese and J.C. Zarnecki, Physical properties of Titan's surface at the Huygens landing site from the Surface Science Package Acoustic Properties sensor (API-S), *Icarus* Vol. 185, 457-465, 2006.
8. L. Ksanfomality, N. V. Goroschkova, V. Khondryev, Wind Velocity near the surface of Venus from Acoustic Measurements, *Cosmic Research* Vol. 21, 161-167, 1983.
9. L. V. Ksanfomality, E. L. Scarf, F. Taylor, The Electrical Activity of the Atmosphere of Venus, in Hunten D M (ed) Venus, University of Arizona Press, 1983.
10. L. V. Ksanfomaliti, N.V. Goroshkova, M.K. Naraeva, A.P. Suvorov, V.K. Khodyrev, L.V. Yabrova, Acoustic measurements of the wind velocity at the Venera 13 and Venera 14 landing sites. *Sov. Astron. Lett.*, Vol. 8(4), 227-229, 1982.
11. G. Clark, Listening for the Buzz of Thin Windy Air, 991014, (http://www.space.com/news/mars_microphone991014.html), 1999.
12. G. T. Delory, J. Luhmann, L. Friedman, B. Betts, Development of the first audio microphone for use on the surface of Mars. *Journal of the Acoustical Society of America*, Vol. 121(5), 3116, 2007 (abstract only).
13. T. G. Leighton, The use of acoustics in space exploration, *ISVR Technical Report* 314, 2007.
14. <http://www-pw.physics.uiowa.edu/space-audio/>

15. P. De Bernardis, P. A. R. Ade, J. J. Bock, J. R. Bond, J. Borrill, A. Boscaleri, K. Coble, B. P. Crill, G. De Gasperis, P. C. Farese, P. G., Ferreira, K. Ganga, M. Giacometti, E. Hivon, V. V. Hristov, A. Iacoangeli, A. H. Jaffe, A. E. Lange, L. Martinis, S. Masi, P. V. Mason, P. D. Mauskopf, A. Melchiorri, L. Miglio, T. Montroy, C. B. Netterfield, E. Pascale, F. Piacentini, D. Pogosyan, S. Prunet, S. Rao, G. Romeo, J. E. Ruhl, F. Scaramuzzi, D. Sforna, N. Vittorio, A flat Universe from high-resolution maps of the cosmic microwave background radiation, *Nature* Vol. 404, 955-959, 2000.
16. J. G. Cramer, BOOMERanG and the Sound of the Big Bang, *Analog Science Fiction & Fact Magazine; Issue 01/01, Article AltVw104* (January), 2001.
17. M. C. Bento, O. Bertolami, A. A. Sen, Generalized Chaplygin gas and cosmic microwave background radiation constraints, *Phys. Rev. D* Vol. 67, 063003-1 to 063003-5, 2003.
18. <http://staff.washington.edu/seymour/altvw104.html>
19. U. Lee, Acoustic oscillations of Jupiter, *The Astrophysical Journal*, Vol. 405, 359-374, 1993.
20. R. W. Noyes, S. Jha, S. G. Korzennik, M. Krockenberger, P. Nisenson, T. M. Brown, A planet orbiting the star ρ Coronae Borealis, *The Astrophysical Journal*, Vol. 483, L111–L114, 1997.
21. F. Bouchy, M. Bazot, N. C. Santos, S. Vauclair, D. Sosnowska, *Asteroseismology of the planet-hosting star μ Arae. I. The acoustic spectrum. Astronomy and Astrophysics*, Vol. 440, 609-614, 2005.
22. Y. Elsworth, R. Howe, G. R. Isaak, C. P. Mcleod, R. New, Variation of low-order acoustic solar oscillations over the solar cycle, *Nature* Vol. 345, 322–324, 1990.
23. W. Rammacher, P. Ulmschneider, Acoustic waves in the solar atmosphere. IX- Three minute pulsations driven by shock overtaking. *Astron. and Astrophys.* Vol. 253, 586-600, 1992.
24. F. Verheest, Are weak dust-acoustic double layers adequately described by modified Korteweg-de Vries equations? *Physica Scripta*, Vol. 47, 274-277, 1993.
25. J. B. Pieper, J. Goree, Dispersion of Plasma Dust Acoustic Waves in the Strong-Coupling Regime, *Physical Review Letters*, Vol. 77, 3137-3140, 1996.
26. M. Rosenberg, G. Kalman, Dust acoustic waves in strongly coupled dusty plasmas, *Physical Review E*, Vol. 56, 7166-7173, 1997.
27. R. L. Merlino, Current-Driven Dust Ion Acoustic Instability in a Collisional Dusty Plasma, *IEEE Transactions on Plasma Science*, Vol. 25, 60-65, 1997.
28. P. K. Shukla, Dust acoustic wave in a thermal dusty plasma, *Physical Review E*, Vol. 61, 7249-7251, 2000.
29. M. R. Gupta, S. Sarkar, S. Ghosh, M. Debnath, M. Khan, Effect of nonadiabaticity of dust charge variation on dust acoustic waves: Generation of dust acoustic shock waves, *Physical Review E*, Vol. 63, 046406-1 - 046406-9, 2001.
30. T. G. Leighton, D. C. Finfer, P. R. White, Ocean acoustic circumpropagation in the ice seas of Europa, *ISVR Technical Report No. 319*, 2007.
31. T. G. Leighton, D. C. Finfer, P. R. White, The problems with acoustics on a small planet, *Icarus*, Vol. 193(2), 649-652, 2008.
32. M. S. Marley, Seismological consequences of the collision of shoemaker-Levy/9 with Jupiter, *Astrophysical Journal, Part 2 - Letters*, vol. 427, no. 1, p. L63-L66, 1994.

33. A. P. Ingersoll, H. Kanamori, Waves from the collisions of comet Shoemaker–Levy 9 with Jupiter, *Nature* Vol. 374, 706-708, 2002.
34. C. M. Walter, M. S. Marley, D. M. Hunten, A. L. Sprague, W. K. Wells, A. Dayal, W. F. Hoffman, M. V. Sykes, L. K. Deutsch, G. G. Fazio, J. L. Hora, A Search for Seismic Waves from the Impact of the SL/9 R Fragment. *Icarus* Vol. 121(2), 341-350, 1996.
35. T. G. Leighton, What is ultrasound? *Progress in Biophysics and Molecular Biology*, Vol. 93, Issues 1-3 , 3-83 (esp. pp. 60-64), 2007.
36. A. Petculescu, R. M. Lueptow, Fine-tuning molecular acoustic models: sensitivity of the predicted attenuation to the Lennard-Jones parameters, *Journal of the Acoustical Society of America*, Vol. 117, 175-184, 2004.
37. Y. Dain, R. M. Lueptow, Acoustic attenuation in three-component gas mixtures – theory, *Journal of the Acoustical Society of America*, Vol. 109, 1955-1964, 2001.
38. A. Petculescu, R. M. Lueptow, Atmospheric acoustics of Titan, Mars, Venus, and Earth, *Icarus*, Vol. 186(2) 413-419, 2007.
39. J. Williams, I. J. McEwan, A Generalized Planetary Acoustic, Ray-tracing Model with Example Application to Bolide Detection on Mars. *Eos Trans. AGU*, Vol. 83(47), *Fall Meet. Suppl.*, Abstract P11A-0351, 2002 (abstract only).
40. Jean-Pierre Williams and Ian McEwan. The propagation of sound in planetary atmospheres and its application to bolide detection. *Journal of the Acoustical Society of America*, Vol., 121(5), pp. 3116, 2007 (abstract only).
41. A. D. Hanford, L. N. Long, V. W. Sparrow, The propagation of sound on Titan using the direct simulation Monte Carlo. *Journal of the Acoustical Society of America*, Vol., 121(5), pp. 3116, 2007 (abstract only).
42. R. L. Kovach, C. F. Chyba, Seismic Detectability of a Subsurface Ocean on Europa, *Icarus* Vol. 150, 279–287, 2001.
43. S. Lee, M. Zanolin, A. M. Thode, R. T. Pappalardo, N. C. Makris, Probing Europa’s interior with natural sound sources, *Icarus* Vol. 165, 144–167, 2003.
44. T. G. Leighton, P. R. White, D. C. Finfer, The Sounds of Seas in Space. *Proceedings of the International Conference on Underwater Acoustic Measurements, Technologies and Results*, J.S. Papadakis and L. Bjorno, eds. (Crete) 833-840, 2005.
45. P. M. Schenk, W. B. McKinnon, Fault offsets and lateral crustal movement on Europa: Evidence for a mobile ice shell, *Icarus*, Vol. 79, 75-100, 1989.
46. G. V. Hoppa, B. R. Tufts, R. Greenberg, P. E. Geissler, Formation of cycloidal features on Europa. *Science* Vol. 285, 1899–1902, 1999.
47. S. Lee, R. T. Pappalardo, N. C. Makris, Mechanics of tidally driven fractures in Europa’s ice shell, *Icarus* Vol. 177, 367–379, 2005.
48. F. Nimmo, P. Schenk, Normal faulting on Europa: Implications for ice shell properties, *J. Struct. Geol.*, Vol. 28, 2194–2203, 2006.
49. T. J. Ringrose, M. C. Towner, J. C. Zarnecki, Convective vortices on Mars: a reanalysis of Viking Lander 2 meteorological data, sols 1–60. *Icarus* Vol. 163, 78-87, 2003.
50. F. A. Farrelly, A. Petri, L. Pitolli, G. Pontuale, In situ acoustic-based analysis system for physical and chemical properties of the lower Martian atmosphere. *Planetary and Space Science*, Vol. 52, 125-131, 2004.

51. E. R. Stofan, C. Elachi, J. I. Lunine, R. D. Lorenz, B. Stiles, K. L. Mitchell, S. Ostro, L. Soderblom, C. Wood, H. Zebker, S. Wall, M. Janssen, R. Kirk, R. Lopes, F. Paganelli, J. Radebaugh, L. Wye, Y. Anderson, M. Allison, R. Boehmer, P. Callahan, P. Encrenaz, E. Flamini, G. Francescetti, Y. Gim, G. Hamilton, S. Hensley, W. T. K. Johnson, K. Kelleher, D. Muhleman, P. Paillou, G. Picardi, F. Posa, L. Roth, R. Seu, S. Shaffer, S. Vetrella, R. West, The lakes of Titan. *Nature*, Vol. 445, 61-64, 2007.
52. T. Tokano, C. P. McKay, F. M. Neubauer, S. K. Atreya, F. Ferri, M. Fulchignoni, H. B. Niemann, Methane drizzle on Titan, *Nature*, Vol. 442, 432-435, 2006.
53. C. Sotin, Titan's lost seas found. *Nature*, Vol. 445(7123), 29-30, 2007.
54. K. Zahnle, L. Dones, H. F. Levison, Cratering rates on the Galilean satellites. *Icarus* Vol. 136, 202-222, 1998.
55. T. G. Leighton, P. R. White, D. C. Finfer, E. J. Grover, The sounds of seas in space: the 'waterfalls' of Titan and the ice seas of Europa, *Proceedings of the Institute of Acoustics*, vol. 28(1), 75-97, 2006.